

# Limiting magnitude, $\tau$ , $t_{\text{eff}}$ , and image quality in DES Year 1

Eric H. Neilsen, Jr.<sup>\*</sup>, Gary Bernstein,<sup>†</sup> Robert Gruendl<sup>‡§</sup>, Stephen Kent<sup>¶</sup>

March 3, 2016

## Abstract

The Dark Energy Survey (DES) is an astronomical imaging survey being completed with the DECam imager on the Blanco telescope at CTIO. After each night of observing, the DES data management (DM) group performs an initial processing of that night's data, and uses the results to determine which exposures are of acceptable quality, and which need to be repeated. The primary measure by which we declare an image of acceptable quality is  $\tau$ , a scaling of the exposure time. This is the scale factor that needs to be applied to the open shutter time to reach the same photometric signal to noise ratio for faint point sources under a set of canonical good conditions. These conditions are defined to be seeing resulting in a PSF full width at half maximum (FWHM) of  $0.9''$  and a pre-defined sky brightness which approximates the zenith sky brightness under fully dark conditions. Point source limiting magnitude and signal to noise should therefore vary with  $\tau$  in the same way they vary with exposure time. Measurements of point sources and  $\tau$  in the first year of DES data confirm that they do.

In the context of DES, the symbol  $t_{\text{eff}}$  and the expression "effective exposure time" usually refer to the scaling factor,  $\tau$ , rather than the actual effective exposure time; the "effective exposure time" in this case refers to the effective duration of one second, rather than the effective duration of an exposure.

<sup>\*</sup>Fermi National Accelerator Laboratory, P. O. Box 500, Batavia, IL 60510, USA

<sup>†</sup>Department of Physics and Astronomy, University of Pennsylvania, Philadelphia, PA 19104, USA

<sup>‡</sup>Department of Physics, University of Illinois, Urbana, IL 61801, USA

<sup>§</sup>National Center for Supercomputing Applications, 1205 West Clark St., Urbana, IL 61801, USA

<sup>¶</sup>Fermi National Accelerator Laboratory, P. O. Box 500, Batavia, IL 60510, USA

## 1 Introduction

The Dark Energy Survey (DES) is an imaging survey of  $\sim 5000^\circ$  of the southern galactic cap, scheduled to take 525 nights of observing with the DECam camera [Flaugher et al.(2015)] on the Blanco telescope at Cerro Tololo Inter-American Observatory, distributed over 5 years [Flaugher(2005)] [Frieman (2014)]. The completed survey will include five exposures, one in each of five filters, for each of 16,045 pointings distributed over the footprint, for a total of 80,225 exposures.

To make optimal use of conditions that vary with time, observing software schedules each exposure shortly before it is observed. The scheduling software, *obstac*, bases its selection on a variety of survey state and environmental parameters, including completion status, seeing, and sky brightness conditions [Neilsen & Annis(2014)]. After each night of observing, the DES data management team (DES-DM) [Mohr et al.(2012)] processes the data for that night to generate initial catalogs, sky brightness estimates, point spread function (PSF) full-width at half maximum (FWHM) measurements, and atmospheric opacity estimates for each exposure. From these, data management determines which exposures need to be repeated [Diehl et al.(2014)].

The observing team then updates the database from which *obstac* selects exposures so that it can schedule exposures that need to be re-observed.

Several factors may cause an image to fail to meet quality requirements. Among the most important of these is the depth: the brightness at which the magnitudes of objects can be detected and flux measured with a given signal to noise ratio.

## 2 The effective exposure time

The measured signal from an object in a DES image is proportional to its flux above the atmosphere,  $f$ , the atmospheric transmission,  $\eta$ , and the exposure time,  $t$ . The noise from the background in the measurement of a point source

is proportional to the square root of the sky brightness (the product of the flux from the sky,  $b$ , and the exposure time  $t$ ):  $\sqrt{bt}$ ; and area over which the signal is spread, itself proportional to the image point spread function full width at half-maximum (PSF FWHM). Near the detection limit, where the depth of the image is measured, this noise dominates the noise overall. The signal to noise ratio, SNR, therefore varies as:

$$\text{SNR} \propto \frac{f\eta t}{\text{FWHM}\sqrt{bt}} = f \times \sqrt{\frac{\eta^2}{\text{FWHM}^2 b}} \times t \quad (1)$$

We define a quantity, the effective exposure time ratio  $\tau$ , in terms of a canonical set of conditions, with  $\eta = 1$ ,  $\text{FWHM} = 0.9''$ , and a sky brightness  $b_{\text{dark}}$  representative of zenith dark sky:

$$\tau \equiv \frac{\eta^2 \times (0.9'')^2 \times b_{\text{dark}}}{\text{FWHM}^2 b} = \eta^2 \left( \frac{\text{FWHM}}{0.9''} \right)^{-2} \left( \frac{b}{b_{\text{dark}}} \right)^{-1} \quad (2)$$

This scale factor  $\tau$  can be used to calculate an effective exposure time as  $\tau \times \text{EXPTIME}$ . However, in the context of DES, the symbol  $t_{\text{eff}}$  and the expression "effective exposure time" usually refer to the scaling factor,  $\tau$ , rather than the actual effective exposure time; the "effective exposure time" in this case refers to the effective duration of a one second exposure, rather than the effective duration of the full exposure.

The SNR of a point source then varies as  $\sqrt{\tau}$ :

$$\text{SNR} \propto f \times \sqrt{t \times \tau} \quad (3)$$

The ratio of the SNR values for point sources in two different exposures is then:

$$\frac{\text{SNR}_1}{\text{SNR}_2} = \frac{f_1}{f_2} \sqrt{\frac{\tau_1 \times t_1}{\tau_2 \times t_2}} \quad (4)$$

The exact value of a "fully dark sky" varies with time, so a canonical representative value is used. Table 1 shows these canonical values in  $\text{mag}/\square''$ , by filter.

Table 1: The canonical sky brightness values used for  $\tau$ .

filter	$b_{\text{dark}}$ ( mag./ $\square''$ )
g	22.23
r	21.40
i	20.18
z	19.04
Y	18.12

### 3 Depth of individual exposures

The magnitude is defined to be linear in log flux:

$$m = m_0 - 2.5 \log_{10}(f) \simeq m_0 - 1.0857 \ln(f) \quad (5)$$

so standard propagation of errors results in a magnitude uncertainty proportional to the inverse SNR:

$$\sigma_m = 1.0857 \frac{\sigma_f}{f} = \frac{1.0857}{\text{SNR}} \quad (6)$$

If point sources in exposures with different  $\tau$  values have the same exposure times,  $t_1 = t_2$ , and uncertainty in magnitude,  $\sigma_{m,1} = \sigma_{m,2}$ , then

$$1 = \frac{\sigma_{m,2}}{\sigma_{m,1}} = \frac{\text{SNR}_1}{\text{SNR}_2} = \frac{f_1}{f_2} \sqrt{\frac{\tau_1}{\tau_2}} \quad (7)$$

so

$$\frac{f_1}{f_2} = \sqrt{\frac{\tau_2}{\tau_1}} \quad (8)$$

and their magnitude should differ by

$$m_1 - m_2 = -2.5 \log \left( \frac{f_1}{f_2} \right) \quad (9)$$

$$= -2.5 \log \left( \sqrt{\frac{\tau_2}{\tau_1}} \right) \quad (10)$$

$$= 1.25 \log \left( \frac{\tau_1}{\tau_2} \right) \quad (11)$$

If we now define the "limiting magnitude" as the magnitude at which we can measure the magnitude of a star with an uncertainty of 0.1 mag. (roughly corresponding to  $\text{SNR}=10$ ), and define  $m_0$  as the limiting magnitude where  $\tau=1$ , then the limiting magnitude should be related to  $\tau$  as:

$$m_{\text{lim}} = m_0 + 1.25 \log \tau \quad (12)$$

The DES data management processing of year 1 of DES data produces values of  $\tau$  for each year 1 exposure and catalogs of objects in each exposure. These catalogs include magnitudes and magnitude uncertainties measured using several methods [Bertin & Arnouts(1996)] [Bertin(2011)]. (All magnitudes and uncertainties reported here were measured using PSF fitting.)

Data management also combined overlapping exposures into co-added exposures, and generated catalogs including magnitudes and corresponding uncertainties from these co-added images as well.

To test the correspondence between  $\tau$  and limiting magnitude in individual exposures, we select a sample of point

sources near the  $10\sigma$  limiting magnitude. The flux uncertainty in a source at the  $10\sigma$  detection limit will be a tenth of its flux, and so have a magnitude uncertainty near 0.1 (by equation 6); the points in figure 1 represent point sources with magnitude uncertainties between 0.095 and 0.105 in individual exposures.

The horizontal axis marks the  $\tau$  of the exposures in which these detection occurred, and the vertical axis shows the median magnitude of these stars as measured in each co-added image. Magnitudes from co-added images are used for the vertical axis rather than magnitudes from individual exposures because they are measured with higher SNR there; the measurements from individual exposures have only an SNR of 10, by construction.

Over-plotted lines show equation 12 with  $m_0$  set to the median difference between  $m_{\text{lim}}$  and  $1.25 \log \tau$ . Figure 2 shows the dispersion of the measured magnitudes around this fit. The positions of these distributions represent the value of  $m_0$  in equation 12, and are listed in column 1 of table 2.

The spread in these distributions arises both from the effectiveness of using  $\tau$  for such an estimation, and inherent uncertainty due to estimating the limiting magnitude using the magnitudes of stars near the detection limit.

Table 2: The measured values of  $m_0$  from equation 12 (median ( $m_{\text{lim}} - 1.25 \log \tau$ )) for  $10\sigma$  detections, and the corresponding inter-quartile range (difference between the third and first quartiles) of the distribution of these values over exposures, estimates from catalog-level co-added stars, and co-add molygons, respectively.

band	exposure	catalog	image
	$10\sigma$ $m_0$ (IQR)	co-add $10\sigma$ $m_0$ (IQR)	co-add $10\sigma$ $m_0$ (IQR)
g	23.41 (0.14)	23.22 (0.20)	23.48 (0.10)
r	23.09 (0.07)	23.04 (0.17)	23.22 (0.10)
i	22.48 (0.10)	22.51 (0.16)	22.64 (0.10)
z	21.82 (0.08)	21.88 (0.13)	22.09 (0.11)
Y	20.35 (0.09)	20.41 (0.24)	20.52 (0.11)

## 4 Depth of co-added images

### 4.1 $\tau$ in coadded images

Given a set of independent magnitude estimates of a point source with varying uncertainties (variances), a combined estimate with minimal uncertainty can be obtained using a weighted mean, where each measurement is weighted by its inverse square uncertainty (inverse variance). The resultant

uncertainty is then:

$$\sigma_m^2 = \frac{1}{\sum_i 1/\sigma_{m,i}^2} \quad (13)$$

so

$$\frac{1}{\text{SNR}^2} = \frac{1}{\sum_i \text{SNR}_i^2}. \quad (14)$$

By equation 3,  $\text{SNR}^2 \propto \tau \times t$ , so the product  $\tau \times t$  adds linearly, as if it were an exposure time itself:

$$\tau \times t = \sum_i \tau_i \times t_i. \quad (15)$$

In the DES wide survey, for which all exposures of a given filter have the same exposure time:

$$\tau = \sum_i \tau_i. \quad (16)$$

### 4.2 catalog co-adds

The DES Y2Q1 catalog [Drlica-Wagner et al. (2016)] combines single-epoch measurements of objects found in the first two years of observing into a single catalog, producing magnitude estimates and uncertainties combining the magnitudes measured in each exposures in which they are detected. Because this catalog includes only objects detected in individual exposures, the limiting magnitude for this catalog will repeat the limiting magnitudes of individual exposures. However, the SNR of the combined magnitudes will reflect the SNR contributions of each image in which the object was detected. Objects whose magnitudes are measured with  $\text{SNR} = 10$  in the co-add catalog will have been present at lower SNR in the detection images, often at low enough SNR not to have been detected at all, and therefore not included in the catalog. To create a catalog of objects with constant SNR in the co-add catalog, we therefore need to consider objects in the co-add catalog whose SNR is high enough to have been detected in individual exposures included in the co-adds.

For sky-noise dominated measurements of object magnitudes, the SNR is proportional to the flux. A detection with an arbitrary SNR therefore has a flux  $\frac{\text{SNR}}{10}$  times greater than one with  $\text{SNR} = 10$ , and so magnitude offset will be:

$$m_0 - m = 2.5 \times (\log \text{SNR} - 1). \quad (17)$$

To generate a collection of measurements comparable to the DES year 1 single exposure sample described earlier, I extract a sample of stars randomly selected from stars in the Y2Q1 data release for which all contributing exposures were taken in year 1; and with a PSF fit magnitude uncertainty

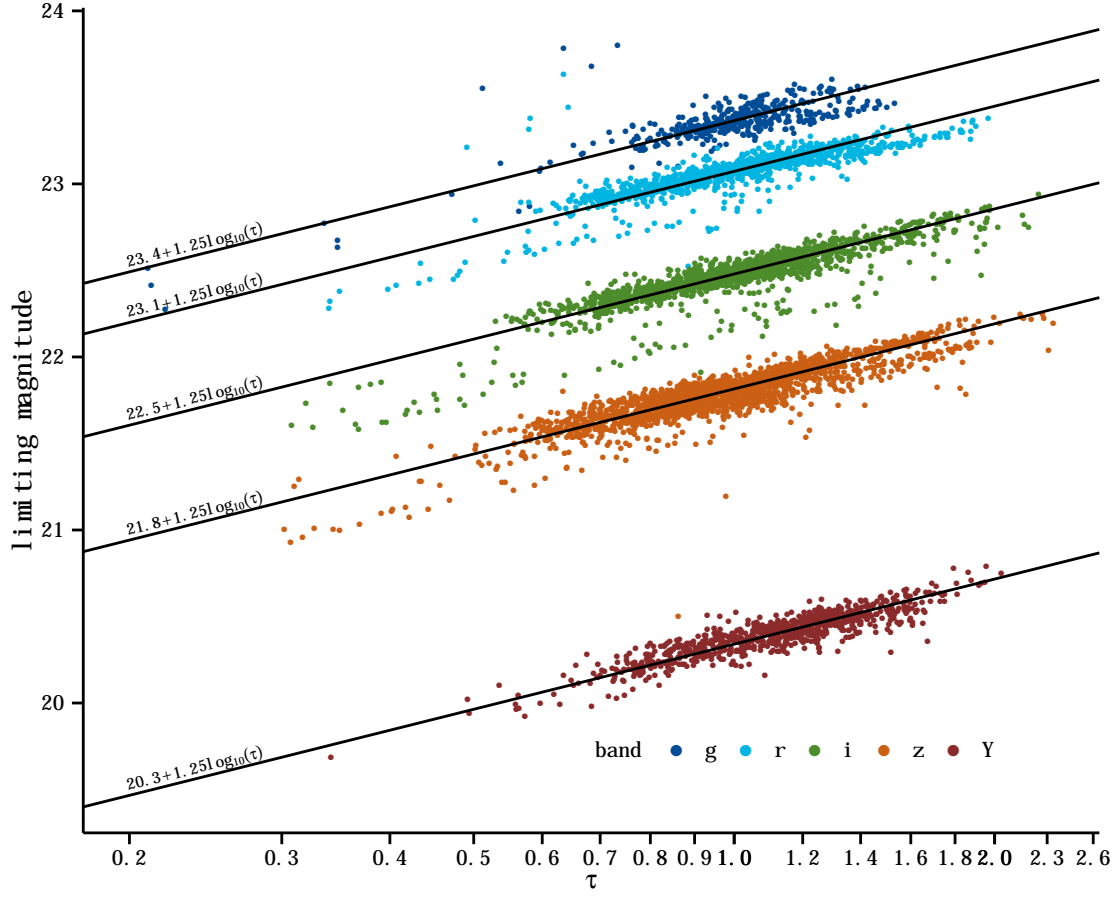


Figure 1: The measured limiting magnitude (at  $\sigma_m=0.1$ ) in each DES year 1 exposure as a function of  $\tau$ , with best fits to equation 12.

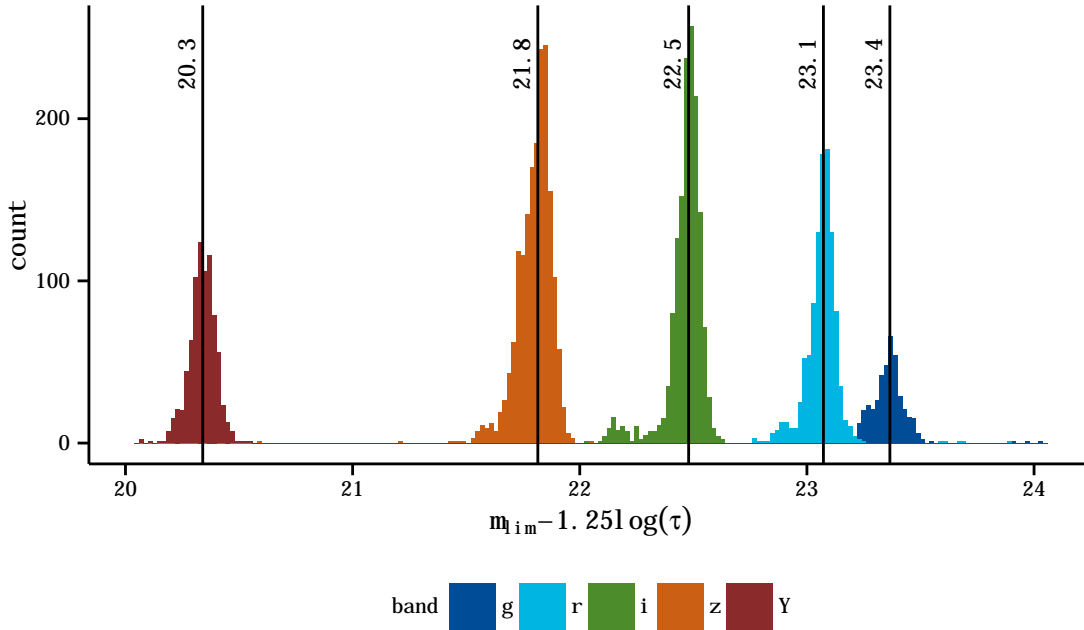


Figure 2: The difference between the limiting magnitude of exposures estimated using the median of stars with magnitude uncertainties of 0.1 mag and the limits as estimated by  $\tau$ , offset by a filter-dependent zero-point.

between 0.005 and 0.015, corresponding to  $\text{SNR} \simeq 100$ .  $m_0$  can then be derived from each following equation 17.

While the sample of stars evaluated here is selected based on uncertainties in the Y2Q1 catalog, the magnitudes themselves are taken from the Y1A1 image-level co-add catalogs (see below) to ensure the resultant values for  $m_0$  use the same un-dereddened photometric calibrations, and so are directly comparable with the values used for individual exposures and image-level measurements of  $m_0$ .

Figure 3 plots  $m_0$  against  $\tau$  for these stars, analogous to figure 1, but plotting densities of stars rather than individual points. Figure 4 shows the distribution of values measured for  $m_0$ , analogous to figure 2. The positions of these distributions represent the value of  $m_0$  in equation 12, and are listed in column 2 of table 2.

Note the lack of apparent bimodal structure in figure 4, in contrast with figure 2.

### 4.3 image co-adds

DES data release Y1A1 organizes the survey area into "molygons", areas covered by a uniform set of exposures [Swanson et al.(2008)]. A total  $\tau$  can therefore be calculated for each molygon, and this  $\tau$  corresponds to all

measurements of stars within than molygon.

Figure 5 plots the co-add magnitude (as measured by PSF fitting) of a random sample of stars that have an uncertainty in PSF magnitude between 0.095 and 0.105 against the measured the sum of the  $\tau$  values for the corresponding molygon, with equation 12 overplotted in black. Column 3 of table 2 shows the median difference between  $m_{\text{lim}}$  and  $1.25 \log \tau$  for a  $10 \sigma$  limiting magnitude, and column 4 the corresponding IQR for the distribution over molygons.

Figure 6 shows the distribution of differences between limiting magnitudes as estimated using the magnitudes of stars for which  $\sigma_m = 0.1$ , and  $1.25 \log \tau$ , corresponding to figure 1 but for the case of molygons rather than individual exposures. Note again the lack of apparent bimodal structure, in contrast with figure 2.

Because the photometry from the image-level co-add catalog is measured from co-added images, the point sources in individual images cannot be measured independently based on their PSFs, so equation 16 is an upper limit on  $\tau$  rather than an identity.

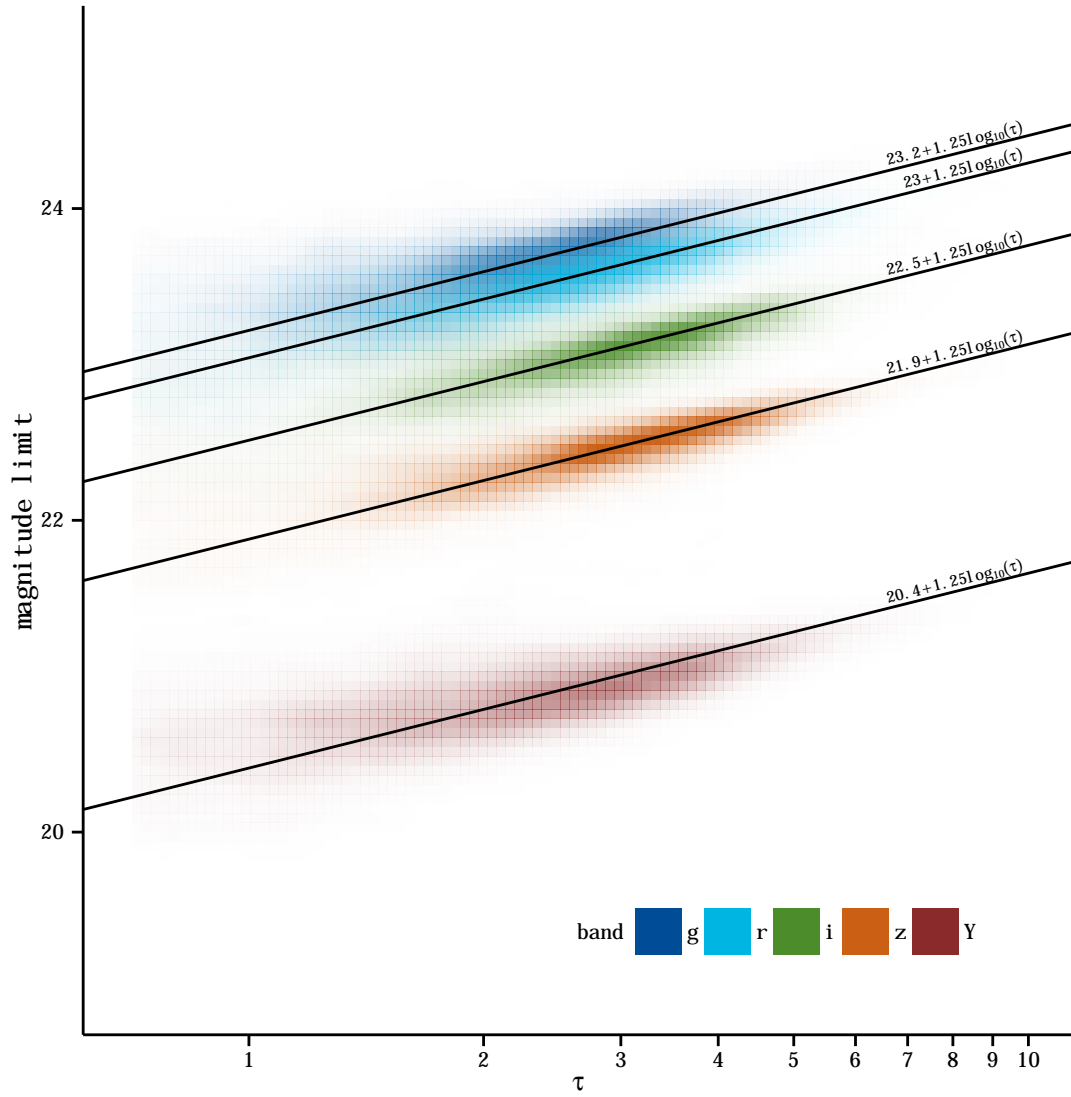


Figure 3: The limiting magnitudes (at  $\sigma_m=0.1$ ) estimated using a random sample of  $\sigma_{\text{MAG\_PSF}} \simeq 0.01$  stars in the Y2Q1 catalog, as a function of  $\Sigma \tau$ , with best zero-point fits to equation 12.

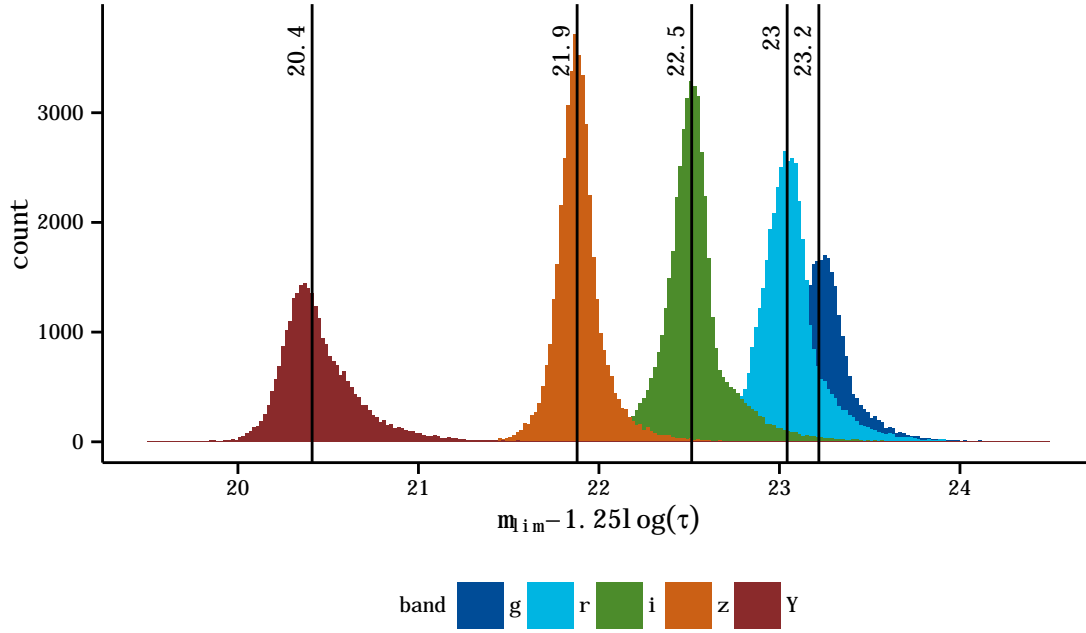


Figure 4: The difference between the estimated magnitude limits as estimated by  $\sum_i \tau$ , offset by a filter-dependent zero-point. Table 2 shows the median and IQR for these distributions. Note the lack of apparent bimodal structure, in contrast with figure 2.

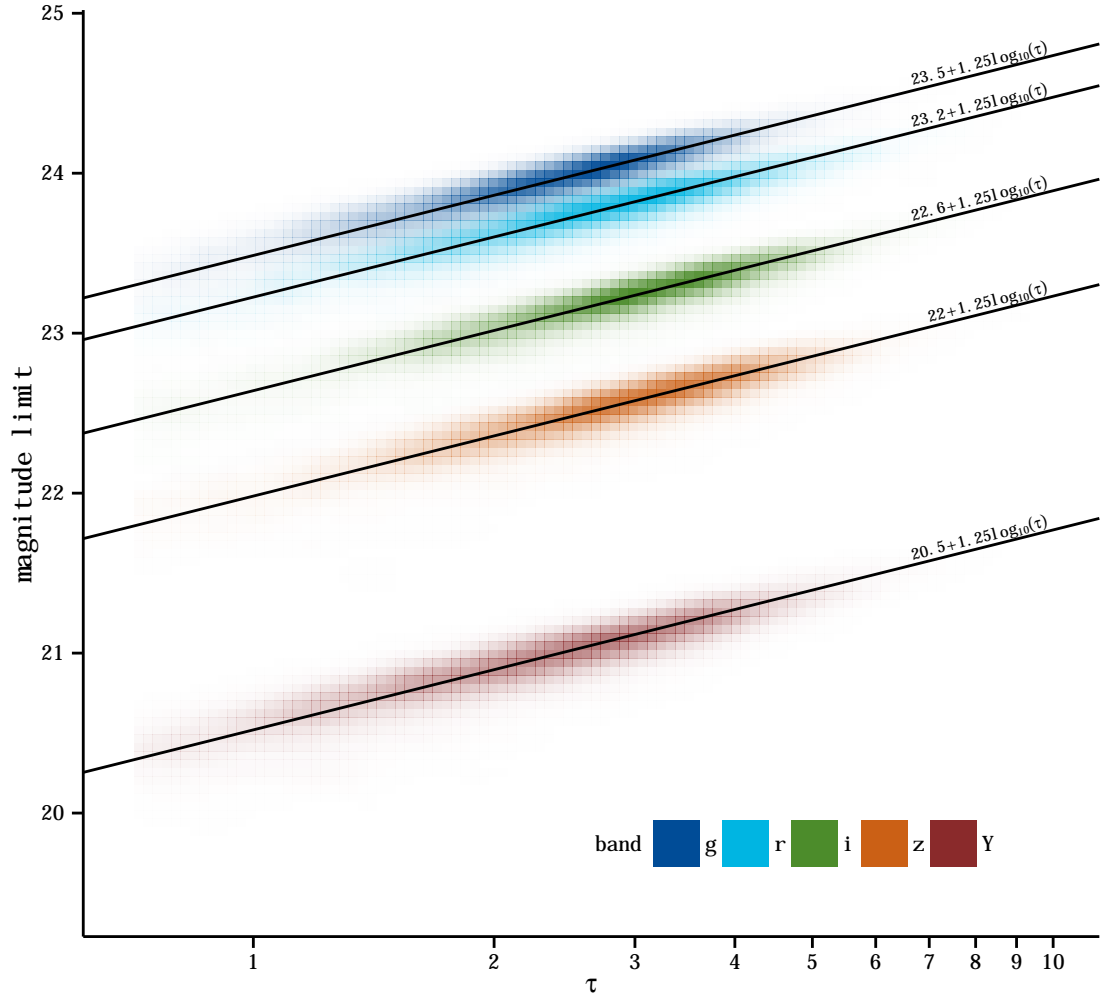


Figure 5: The measured limiting magnitude (at  $\sigma_m=0.1$ ) in a random sample of year 1 co-add molygons, as a function of  $\Sigma \tau$ , with best fits to equation 12.



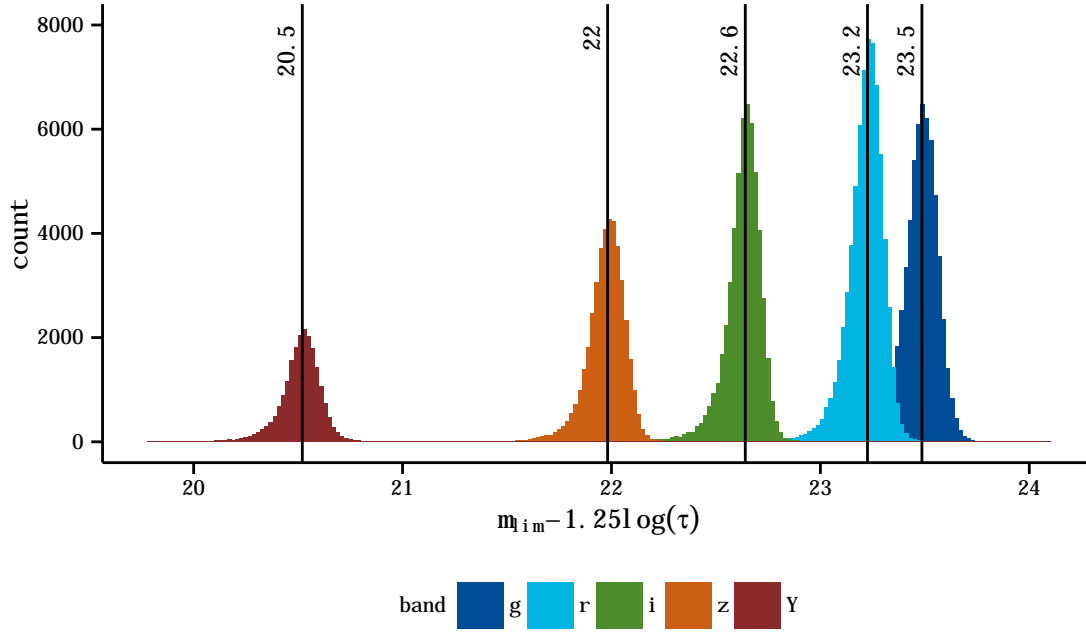


Figure 6: The difference between the limiting magnitude of molygons estimated using the median of stars with magnitude uncertainties of 0.1 mag and the limits as estimated by  $\sum_i \tau$ , offset by a filter-dependent zero-point. Table 2 shows the median and IQR for these distributions. Note the lack of apparent bimodal structure, in contrast with figure 2.

## 5 Discussion and conclusion

The limiting magnitude, as estimated using the magnitudes of stars near the detection limits, appears to vary as expected using  $\tau$ ;  $\tau$  appears to be an adequate measure for image quality for the purposes of repeating exposures spoiled by poor conditions.

The power of this test is limited by the use of stars near the detection limit to estimate the detection limit. However, several mysterious features are apparent:

- in single exposures in most filters, there appears to be a secondary peak in  $m_{lim} - \tau$ , indicating that in some exposures the limiting magnitude is a few tenths of a magnitude brighter than would be estimated using  $\tau$ . This secondary peak is missing in corresponding distributions in both catalog and image-level co-adds.
- The zero-point in equation 12 appears to be 0.1-0.2 magnitudes fainter in image-level co-added images than either single exposures or catalog-level co-added magnitudes, which is opposite of the sense one would expect given the limitations inherent in co-adding exposures with different PSFs.<sup>1</sup>

## References

- [Bertin & Arnouts(1996)] Bertin, E., & Arnouts, S. 1996, *Astronomy and Astrophysics, Supplement*, 117, 393
- [Bertin(2011)] Bertin, E. 2011, *Astronomical Data Analysis Software and Systems XX*, 442, 435
- [Diehl et al.(2014)] Diehl, H. T., Abbott, T. M. C., Annis, J., et al. 2014, *Proc. SPIE*, 9149, 91490V
- [Drlica-Wagner et al. (2016)] Drlica-Wagner, A., Bechtol, K., Rykoff, E. S., et al. 2016 *ApJ* accepted, arXiv:1508:03622
- [Flaugher(2005)] Flaugher, B. 2005, *International Journal of Modern Physics A*, 20, 3121
- [Flaugher et al.(2015)] Flaugher, B., Diehl, H. T., Honscheid, K., et al. 2015, arXiv:1504.02900
- [Frieman (2014)] Frieman, J. 2014, *Physics Today*, 67, 4
- [Mohr et al.(2012)] Mohr, J. J., Armstrong, R., Bertin, E., et al. 2012, *Proc. SPIE*, 8451, 84510D
- [Neilsen & Annis(2014)] Neilsen, E., & Annis, J. 2014, *Astronomical Data Analysis Software and Systems XXIII*, 485, 77
- [Swanson et al.(2008)] Swanson, M. E. C., Tegmark, M., Hamilton, A. J. S., & Hill, J. C. 2008, *Monthly Notices of the RAS*, 387, 1391

## Acknowledgments

Funding for the DES Projects has been provided by the U.S. Department of Energy, the U.S. National Science Foundation, the Ministry of Science and Education of Spain, the Science and Technology Facilities Council of the United Kingdom, the Higher Education Funding Council for England, the National Center for Supercomputing Applications at the University of Illinois at Urbana-Champaign, the Kavli Institute of Cosmological Physics at the University of Chicago, Financiadora de Estudos e Projetos, Fundacao Carlos Chagas Filho de Amparo a Pesquisa do Estado do Rio de Janeiro, Conselho Nacional de Desenvolvimento Cientifico e Tecnologico and the Ministerio da Ciencia e Tecnologia, the Deutsche Forschungsgemeinschaft and the Collaborating Institutions in the Dark Energy Survey.

The Collaborating Institutions are Argonne National Laboratories, the University of California at Santa Cruz, the University of Cambridge, Centro de Investigaciones Energeticas, Medioambientales y Tecnologicas-Madrid, the University of Chicago, University College London, the DES-Brazil Consortium, the Eidgenossische Technische Hochschule (ETH) Zurich, Fermi National Accelerator Laboratory, the University of Edinburgh, the University of Illinois at Urbana-Champaign, the Institut de Ciencies de l'Espai (IEEC/CSIC), the Institut de Fisica d'Altes Energies, the Lawrence Berkeley National Laboratory, the Ludwig-Maximilians Universität and the associated Excellence Cluster Universe, the University of Michigan, the National Optical Astronomy Observatory, the University of Nottingham, the Ohio State University, the University of Pennsylvania, the University of Portsmouth, SLAC National Laboratory, Stanford University, the University of Sussex, and Texas A&M University.

Fermilab is operated by Fermi Research Alliance, LLC under Contract No. De-AC02-07CH11359 with the United States Department of Energy.

<sup>1</sup>The deeper limiting magnitude of the co-added images agrees, however, with the conventional wisdom in the astronomical community.